Intracollisional interference of *R* lines of HD in mixtures of deuterium hydride and helium gas

Magnus Gustafsson and Lothar Frommhold
Physics Department, University of Texas at Austin, Austin, Texas 78712-1081
(Received 30 November 2000; published 18 April 2001)

Line shapes of the $R_0(0)$ and $R_0(1)$ lines in the pure rotational band, and of the $R_1(0)$ and $R_1(1)$ lines in the fundamental band of HD are computed from first principles for HD molecules that interact collisionally with He atoms. Interference of the permanent dipole of the HD molecule and the interaction-induced dipole of HD–He supermolecular complex shapes these profiles. We use the close-coupling scheme for the scattering calculations which take into account the anisotropy of the HD–He interaction potential. Thus rotational level mixing is accounted for in a non-perturbative manner. The treatment is fully quantum mechanical and takes into account single binary collisions between HD and He. Spectral absorption profiles and line shape parameters of the *R*-lines are computed for comparison with existing measurements at 77 K. Agreement between theory and measurements is observed in the low-helium-density limit of the measured absorption as expected.

DOI: 10.1103/PhysRevA.63.052514 PACS number(s): 33.70.Jg, 33.20.Ea

I. INTRODUCTION

Even infrared-inactive gases and mixtures of such gases will absorb infrared radiation in certain broad spectral bands if the gas densities are high enough [1]. The process is usually referred to as interaction-induced absorption because pairs and possibly larger complexes of collisionally interacting atoms or molecules are responsible. Specifically, exchange and dispersion forces and the permanent electric multipoles of molecules induce a transient dipole moment in interacting atoms or molecules which give rise to the various, generally well-known collision-induced absorption bands [2]. Interesting interference effects of permanent and induced dipole components and their associated spectral features may be observed if a collisional complex includes an infrared active molecule and if the induced and permanent dipole moments are of comparable strengths, typically in the 10^{-3} D range.

McKellar [3] discovered such interferences in gaseous deuterium hydride in the fundamental band of HD, and Herman *et al.* [4] gave the first theoretical analysis. Since then new measurements in pure deuterium hydride and in mixtures with rare gases have been published, in both the fundamental band of HD [5–8] and the rotational band in the far infrared [9–11]. Several reviews exist that focus on the collisional interferences of the HD-*X* system, with *X* being another HD molecule or a rare-gas atom [12–16]. It is clear that the line shapes of the HD *R* lines are affected not only by single collisions, the so-called intracollisional interference effect. In general a whole series of subsequent collisions needs to be taken into account, especially near zero-frequency shifts (''intercollisional interferences'') [4,17,18]; these higher-order effects are clearly discernible in the experimental data. However, in the low helium density limit the wings of the profiles of the allowed *R* lines are affected only by single collisions. Our present interest is the line shapes and line-shape parameters of four $R_{v_f}(j_i)$ lines, that is rotovibrational lines of HD with the quantum numbers j_i and j_i+1 of initial and final rotational states, in the pure rotational and fundamental bands, $v_f=0$ and 1, respectively.

Ab initio calculations of the collision-induced absorption profiles of the supermolecular complex H_2-He were previously communicated for the rotational and fundamental bands of the H_2 molecule [19]. For the present study, we use that same close-coupling scheme so that rotational level mixing is directly accounted for—nonperturbatively. The rotational mixing has the effect that all collision-induced dipole components, not just the one with the same symmetry as the permanent dipole of HD, will affect intracollisional interferences. With a nonperturbative treatment one has the advantage that the radiative cross sections are correctly determined even if the rotational mixing is strong. Previous attempts have employed perturbation treatments and in that sense, the close-coupled treatment goes beyond previous work. Recent perturbation calculations, which include the lowest-order rotational level mixing [20], somewhat surprisingly resulted in ''... some major unresolved problems of theory...'' when comparisons with the experimental facts were made. We hope to possibly avoid such problems by the present close-coupled treatment of the HD-He scattering.

II. LINE-SHAPE CALCULATIONS

The Schrödinger equation with an anisotropic interaction potential is integrated using a close-coupling scheme that combines the radiative coupling with the atom-diatom scattering as formulated in Ref. [19]. For the integrations we used the COUPLE computer program developed by Mies, Julienne, and Sando [21].

The Hamiltonian describing the interaction of a rotating and vibrating HD molecule with *N* noninteracting He atoms in the presence of a radiation field $\boldsymbol{E}$ is [18]

$$H=H^{\mathrm{rad}}+H^{\mathrm{mol}}(\boldsymbol{r})-\boldsymbol{\mu}^A(\boldsymbol{r})\cdot\boldsymbol{E}(\omega)+\sum_{i=1}^{N}\left\{-\frac{\hbar^2}{2m}\nabla^2_{\boldsymbol{R}_i}+V(\boldsymbol{r},\boldsymbol{R}_i)-\boldsymbol{\mu}^I(\boldsymbol{r},\boldsymbol{R}_i)\cdot\boldsymbol{E}(\omega)\right\}, \quad (1)$$

where $H^{\rm rad}$ is the Hamiltonian of the isolated radiation field, $H^{\rm mol}$ is the Hamiltonian with eigenvalues $E^{\rm mol}_{vj}$ [22] of the isolated HD molecule, and V is the interaction potential of one HD-He pair which has the reduced mass m. $\boldsymbol{R}_i$ is the vector pointing from the center of mass of the HD molecule to the ith He atom and $\boldsymbol{r}$ is the vector pointing from the H atom to the D atom. $\boldsymbol{\mu}^A$ is the permanent (allowed) electric dipole moment of the diatom and $\boldsymbol{\mu}^I$ is the dipole moment induced by the interaction between a He atom and the diatom. Considering only the contribution from single binary collisions ($N=1$) yields the Hamiltonian,

$$H(\boldsymbol{r},\boldsymbol{R};\omega)=H^{\rm rad}+H^{\rm mol}(\boldsymbol{r})-\frac{\hbar^2}{2m}\nabla^2_{\boldsymbol{R}}+V(\boldsymbol{r},\boldsymbol{R})+V^{\rm rad}(\boldsymbol{r},\boldsymbol{R};\omega), \tag{2}$$

where $V^{\rm rad}$ is the coupling of the HD-He complex with the radiation field. Quantization of the radiation field to a state $|n;\omega\rangle$ with n photons of frequency ω yields

$$H^{\rm rad}|n;\omega\rangle=n\hbar\omega|n;\omega\rangle, \tag{3}$$

and assuming linearly polarized light along the angular-momentum quantization axis $\hat{\boldsymbol{z}}$,

$$V^{\rm rad}(\boldsymbol{r},\boldsymbol{R};\omega)=-\sqrt{\frac{2\pi\hbar\omega\phi}{c}}\{\mu^I_z(\boldsymbol{r},\boldsymbol{R})+\mu^A_z(\boldsymbol{r})\}, \tag{4}$$

where ϕ is the radiation flux in the photon number per area and time.

The total state vector is given by

$$\Psi_\alpha(\boldsymbol{r},\boldsymbol{R};E)\otimes|n;\omega\rangle=\sum_{\alpha' n'} v_{v'j'}(r)\frac{1}{R}F^{n'n}_{\alpha'\alpha}(R;E,\omega) \times Y^{J'M'}_{j'l'}(\hat{\boldsymbol{r}},\hat{\boldsymbol{R}})\otimes|n';\omega\rangle, \tag{5}$$

where $\alpha=(v,j,l,J,M)$. Y^{JM}_{jl} is the vector coupling function,

$$Y^{JM}_{jl}(\hat{\boldsymbol{r}},\hat{\boldsymbol{R}})=\sum_{m_j m_l} C(j,l,J;m_j,m_l,M)Y_{jm_j}(\hat{\boldsymbol{r}})Y_{lm_l}(\hat{\boldsymbol{R}}), \tag{6}$$

corresponding to $\boldsymbol{J}=\boldsymbol{j}+\boldsymbol{l}$: the total angular momentum is the sum of rotational and translational angular momentum. Equations (2) and (5) yield the coupled radial Schrödinger equation [19]

$$\left\{E^{\rm mol}_{v''j''}-\frac{\hbar^2}{2m}\frac{d^2}{dR^2}+\frac{\hbar^2 l''(l''+1)}{2mR^2}+n''\hbar\omega-E\right\} \times F^{n''n}_{\alpha''\alpha}(R;E,\omega)+\sum_{\alpha' n'}\{V_{\alpha''\alpha'}(R)\delta_{n''n'} +V^{\rm rad}_{\alpha''\alpha'}(R;\omega)\delta_{n''\pm1,n'}\}F^{n'n}_{\alpha'\alpha}(R;E,\omega) =0, \tag{7}$$

with coupling matrix elements $V_{\alpha''\alpha'}$ and $V^{\rm rad}_{\alpha''\alpha'}$ which will be defined in Secs. II A and II B. In accordance with the close-coupling scheme, Eq. (7) can be solved for $F^{n''n}_{\alpha''\alpha}$. With energy normalization of the wave functions, the asymptotic boundary condition for $R\to\infty$ is

$$F^{n'n}_{\alpha'\alpha}(R;E,\omega)\sim i\sqrt{\frac{m}{2\pi\hbar^2 k}}\left\{e^{-i(kR-l\pi/2)}\delta_{\alpha'\alpha}\delta_{n'n} -\sqrt{\frac{k}{k'}}e^{i(k'R-l'\pi/2)}S^{n'n}_{\alpha'\alpha}(E,\omega)\right\} \tag{8}$$

for open channels and an exponentially decaying function for closed channels. The channel wave number k is defined by

$$k^2=\frac{2m}{\hbar^2}(E-n\hbar\omega-E^{\rm mol}_{vj}), \tag{9}$$

$$k'^2=\frac{2m}{\hbar^2}(E-n'\hbar\omega-E^{\rm mol}_{v'j'}), \tag{10}$$

and $S^{n'n}_{\alpha'\alpha}$ is the S matrix, from which the desired quantities related to the transition probability between two channels (α,n) and (α',n') are calculated. In principle the summations over α' and n' in Eq. (7) are infinite. However, as we are presently only interested in one-photon absorption we can let the n' summation run only from 0 to 1. We have also truncated the sum over α' by excluding those (closed) channels which hardly affect the radiative transition probabilities at the kinetic energies under consideration.

The binary collision-induced absorption coefficient of a gas mixture of the species with densities ρ_1 and ρ_2, respectively, at the temperature T, is calculated from the S matrix. Let the subscripts i and f designate the initial and final channels, respectively, i.e., channels with one or no photons. For temperatures up to a few hundred kelvin only the vibrational ground state is populated. Thus $v_i=0$ and $v_f=0$ for the rototranslational band and $v_f=1$ for the fundamental band and the absorption coefficient

$$\alpha(\omega,T)=\rho_1\rho_2\frac{1-e^{-\hbar\omega/k_BT}}{\phi h}\sum_{fi}\frac{e^{-E^{\rm mol}_{v_ij_i}/k_BT}}{Z_{\rm roto}} \times\int_0^\infty dE^{\rm kin}_i\frac{e^{-E^{\rm kin}_i/k_BT}}{Z_{\rm trans}}|S_{fi}(E^{\rm kin}_i,\omega)|^2, \tag{11}$$

where $f=(j_f,l_f,J_f)$, $i=(j_i,l_i,J_i)$. There is no summation over the quantum numbers M in Eq. (11) because the coupling matrix elements presented in Secs. II A and II B are both proportional to $\delta_{MM'}$. Accordingly, the coupled equations (7) will be independent of the quantum numbers M. $Z_{\rm trans}$ and $Z_{\rm roto}$ are the translational and rotational partition functions, respectively,

$$Z_{\text{trans}}=\left(\frac{2\pi m k_B T}{h^2}\right)^{3/2}, \tag{12}$$

$$Z_{\text{roto}}=\sum_j (2j+1)e^{-E^{\text{mol}}_{v_i j}/k_B T}, \tag{13}$$

and the initial kinetic energy is

$$E_i^{\text{kin}}=E-\hbar\omega-E^{\text{mol}}_{v_i j_i}. \tag{14}$$

In order to make the calculations of the absorption coefficient (11) less time consuming, two decouplings of the equations (7) are applied according to Ref. [19]. First, the parity, given by $(-1)^{j+l}$ is conserved within the initial and final channels, respectively, while it must change in the radiative transitions. Thus a calculation with even j_i+l_i and odd j_f+l_f is decoupled from one with odd j_i+l_i and even j_f+l_f. Second, the selection rule for the total angular momentum yields the three final total angular momenta

$$J_f=J_i;\quad J_i\pm 1, \tag{15}$$

whose channels can also be decoupled due to the conservation of total angular momentum among the final channels.

We have tried to keep the overall numerical accuracy of the calculation of the spectra at the 1% level or better. To that end we had to answer questions, such as how many closed channels (channels with negative asymptotic kinetic energy) must be included in the integration; how many partial waves to include; and the choice of the grid for the integration over kinetic energy in Eq. (11). We found that inclusion of closed channels with asymptotic kinetic energies as low as $-500\ \text{cm}^{-1}$, or $-10k_BT$, is sufficient. Second, we found it necessary to include total angular-momentum quantum numbers up to $J=22$. Finally, the kinetic energy grid is chosen roughly in the following manner: up to $2k_BT$ our step size is $0.1k_BT$ and from $2k_BT$ to the upper limit, which is $10k_BT$, the step size is $0.5k_BT$. Various trial calculations at the frequencies of interest here seem to confirm a numerical accuracy of the computed line shapes of typically better than 1%.

A. Interaction potential

For an atom-diatom system it is appropriate to expand the interaction potential in Legendre polynomials, according to

$$V(\boldsymbol{r},\boldsymbol{R})=\sum_\gamma V_\gamma(R,r)P_\gamma(\hat{\boldsymbol{r}}\cdot\hat{\boldsymbol{R}}), \tag{16}$$

where the subscripts γ are non-negative integers. Defining coefficients f_γ by

$$\int Y^{JM*}_{jl}(\hat{\boldsymbol{r}},\hat{\boldsymbol{R}})P_\gamma(\hat{\boldsymbol{r}}\cdot\hat{\boldsymbol{R}})Y^{J'M'}_{j'l'}(\hat{\boldsymbol{r}},\hat{\boldsymbol{R}})d\hat{\boldsymbol{r}}d\hat{\boldsymbol{R}} = f_\gamma(j,l,j',l';J)\delta_{JJ'}\delta_{MM'} \tag{17}$$

yields [23]

$$f_\gamma(j,l,j',l';J)=(-1)^{j+j'-J}[(2j+1)(2l+1)(2j'+1)\times(2l'+1)]^{1/2}\begin{Bmatrix} j & l & J\\ l' & j' & \gamma\end{Bmatrix}\begin{pmatrix} l & l' & \gamma\\ 0 & 0 & 0\end{pmatrix}\times\begin{pmatrix} j & j' & \gamma\\ 0 & 0 & 0\end{pmatrix}, \tag{18}$$

where $\{\cdots\}$ are 6-j symbols [24]. Second, defining the radial matrix elements as

$$V_\gamma^{vjv'j'}(R)=\int_0^\infty v^*_{vj}(r)V_\gamma(r,R)v_{v'j'}(r)r^2\,dr \tag{19}$$

allows us to write the interaction potential matrix element as

$$V_{\alpha\alpha'}(R)=\sum_\gamma V_\gamma^{vjv'j'}(R)f_\gamma(j,l,j',l';J)\delta_{JJ'}\delta_{MM'}. \tag{20}$$

The kinetic energy of the collisions of interest here is small enough to prevent nonradiative transitions between different vibrational states and the j dependence of the rotovibrational is assumed to be small. The matrix element (20) can thus be approximated by

$$V_{\alpha\alpha'}(R)=\sum_\gamma V_\gamma^{v}(R)f_\gamma(j,l,j',l';J)\delta_{JJ'}\delta_{MM'}\delta_{vv'}, \tag{21}$$

where for the functions V_γ^v we have adopted the *ab initio* potential surface [25] as given in Ref. [26]. We have included potential components with $\gamma=0$ up to 5 in our lineshape calculations.

B. Radiative coupling

The standard expansion for the collision-induced dipole [27,28]

$$\mu^I_\nu(\boldsymbol{r},\boldsymbol{R})=\frac{4\pi}{\sqrt{3}}\sum_{\lambda L}A^I_{\lambda L}(r,R)Y^{1\nu}_{\lambda L}(\hat{\boldsymbol{r}},\hat{\boldsymbol{R}}), \tag{22}$$

can also be used for the permanent dipole of the molecule [12]. Its only nonvanishing component is the one with $\lambda L=10$ and

$$\mu^A_z(\boldsymbol{r})=\frac{4\pi}{\sqrt{3}}A^A(r)Y^{10}_{10}(\hat{\boldsymbol{r}})=A^A(r)\cos(\theta), \tag{23}$$

and thus

$$V^{\text{rad}}_{\alpha\alpha'}(R;\omega)=-\sqrt{\frac{2\pi\hbar\omega\phi}{c}}\sum_{\lambda L}\{B^{vjv'j'}_{I;\lambda L}(R)+B^{vjv'j'}_A\delta_{\lambda 1}\delta_{L0}\}d_{\lambda L}(j,l,J,j',l',J')\delta_{MM'} \tag{24}$$

with the B functions defined by

$$B^{vjv'j'}(R)=\int_0^\infty v^*_{vj}(r)A(r,R)v_{v'j'}(r)r^2\,dr \qquad (25)$$

and the d coefficients arising from the angular integration [19] by

$$d_{\lambda L}(j,l,J,j',l',J')=\frac{(-1)^{j+l+J}}{\sqrt{3}}\begin{pmatrix} l & l' & L\\ 0 & 0 & 0\end{pmatrix}\begin{pmatrix} j & j' & \lambda\\ 0 & 0 & 0\end{pmatrix}\times\begin{Bmatrix} j' & l' & J'\\ j & l & J\\ \lambda & L & 1\end{Bmatrix}[(2j+1)(2l+1)\times(2j'+1)(2l'+1)(2J+1)(2J'+1)\times(2\lambda+1)(2L+1)]^{1/2}. \qquad (26)$$

For both the permanent and the interaction-induced dipole moment matrix elements we have used *ab initio* data. For the permanent dipole $B_A^{vjv'j'}$ of the HD molecule we used the computed values of Ref. [29]. The interaction-induced dipole function $B_{I;\lambda L}^{vjv'j'}(R)$ is taken from Ref. [30], where it is approximated to be j independent and we have included nine components (λL).

III. RESULTS AND ANALYSIS

In previous experimental analyses a multiparameter Fano profile was used to represent the measured line shapes. In Secs. III A and III B we compare the presently calculated profiles with these measurements in two different ways. First, the Fano profile given in Refs. [31,11] can be extrapolated towards low He densities by simply putting in a small value for the helium density (e.g., 1 amagat) into the Fano formula. The computed points are then compared to this curve. Second, the formula for the Fano profile of Ref. [31,11] can be Taylor expanded towards low He densities. The presently computed points are then fitted to this formula and the fit parameters are compared with the ones obtained from measurement.

A. Line profiles

By means of Eq. (2) in Ref. [31] and the line-shape parameters, also obtained in Ref. [31], comparison between computed and experimental line profiles is done. It is shown for the $R_1(0)$ and $R_1(1)$ lines in Figs. 1 and 2, respectively. In each figure the dots represent the present theory and the experimental profiles [31] are shown as curves for three different He densities: 1, 29.4, and 205 amagats. For the two latter densities measurement of the profile was indeed done while for 1 amagat of He the curve is an extrapolation of the measurement. The wings of the Fano profile may be directly compared with the present line-shape calculations and we see that the calculated values agree well with the experimental curves for the lowest He density. Note that we have not calculated values for smaller detunings than roughly 0.5 cm^{-1} because the numerical integration of the coupled equations (7) becomes unstable as one approaches the resonances.

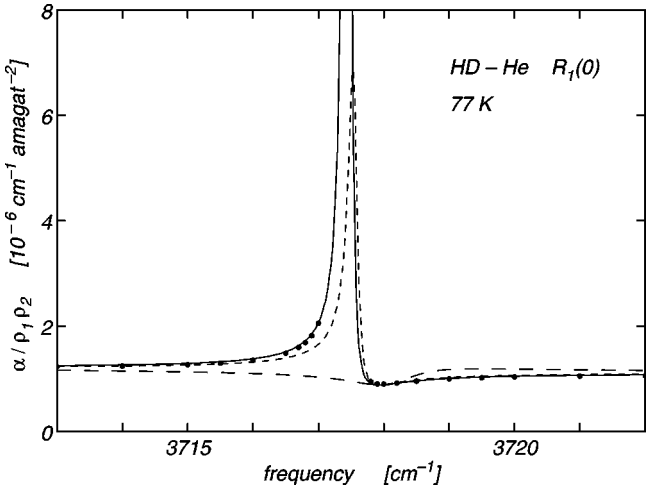

FIG. 1. The absorption coefficient α, normalized by the He and HD gas densities, ρ_1 and ρ_2, respectively, as a function of frequency at the $R_1(0)$ line, and at the temperature of 77 K. Dots represent present calculations. Also shown is the Fano profile, determined experimentally in Ref. [31], for three different helium densities; solid line: 1 amagat; short dashes: 29.4 amagats; long dashes: 205 amagats.

B. Line-shape parameters

We expand the Fano profile given in Refs. [31,11] into a Taylor series in terms of the helium density. Keeping only the terms which are linear in the helium density ρ_1, we obtain the formula

$$\frac{\alpha(\nu)}{\rho_1\rho_2}=\frac{c_0\nu}{2\pi}\left\{\frac{B_0}{(\nu-\nu_0(0))^2}+\frac{4\Delta''I}{\nu-\nu_0(0)}\right\}+a+b\nu. \qquad (27)$$

Here we have also assumed that the linewidth is zero at zero helium density. This must be the case for our model which

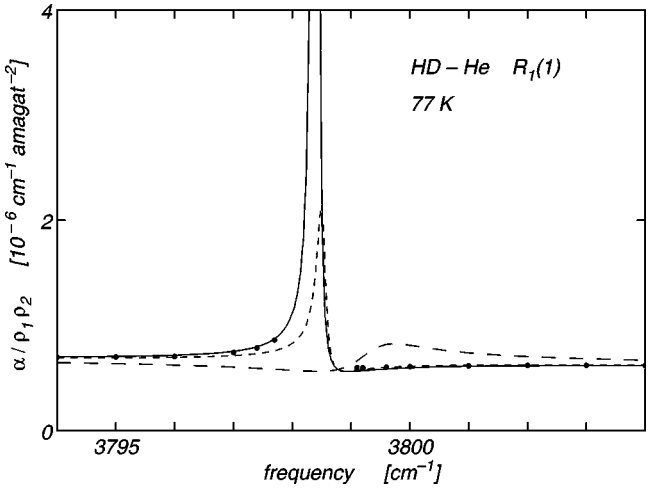

FIG. 2. Same as in Fig. 1 but for the $R_1(1)$ line.

TABLE I. Comparison of calculated and measured Fano parameters. The semiclassical calculations are made using the theory of Ref. [18]. Square brackets indicate powers of ten.

		B_0 (cm^{-1} am^{-1})	$\Delta''I$ (am^{-1})	a (cm^{-1} am^{-2})	b (am^{-2})	$\nu_0(0)$ (cm^{-1})
$R_0(0)$	present work	0.00363	0.00109	0.527 [−7]	0.338[−8]	89.23
	measurement [11]	0.00293(12)	0.0015(3)			
	semiclassical [33]	0.0062	0.00060			
$R_0(1)$	present work	0.00471	0.000837	0.484[−6]	$-0.187E$[−9]	177.84
	measurement [11]	0.00391(11)	0.0013(3)			
	semiclassical [33]	0.0039	−0.000027			
$R_1(0)$	present work	0.00515	−0.00492	0.258[−4]	−0.663[−8]	3717.44
	measurement [31]	0.0056(2)	−0.0059(1)			
	semi-classical [34]	0.0064	−0.00266			
	quantum [20]		−0.0011			
$R_1(1)$	present work	0.00631	−0.00393	0.162[−4]	−0.409[−8]	3798.39
	measurement [31]	0.0062(3)	−0.0055(1)			
	semiclassical [34]	0.0040	0.00079			
	quantum [20]		−0.0003			

does not have any other broadening mechanism than binary collisions of HD and He. Note that Eq. (27) is only used to fit the presently computed points and the singularity at zero detuning does not matter; it could easily be suppressed if desired. For fits of measured absorption profiles one should use a formula with a finite linewidth at zero helium density to account for various broadening mechanisms, e.g., Doppler broadening, natural linewidth, and instrumental broadening. Equation (27) represents the sum of a Lorentzian and a dispersion line shape and the terms $a+b\nu$ are just a base-line correction to model the collision-induced background absorption. The calculated absorption profiles have been fitted to the model, Eq. (27), by adjusting the fit parameters $B_0, \Delta''I, \nu_0(0), a$, and b by means of a nonlinear fit algorithm. The resulting values are presented in Table I for comparison with measurements and the semiclassical theory. B_0 is the broadening parameter, called γ in Ref. [31], and $\Delta''I$ is the asymmetry parameter for the profile. c_0, called $\tilde{\alpha}(0)$ in Ref. [31], is directly related to the permanent dipole matrix element for an R transition, namely [9],

$$c_0=\frac{4\pi^2}{3\hbar c}\,\frac{e^{-E^{\mathrm{mol}}_{v_i j_i}/k_B T}-e^{-E^{\mathrm{mol}}_{v_f j_f}/k_B T}}{Z_{\mathrm{roto}}}(j_i+1)\left|B_A^{v_i j_i v_f j_f}\right|^2, \tag{28}$$

where the factor j_i+1 should be replaced by j_i in case of a P transition and Z_{roto} is defined in Sec. II. The theoretical and experimental values of c_0 are given in Table II. The theoretical values of c_0 were used in our Eq. (27) to obtain the fit parameters given in Table I. Note that the theoretical values of c_0 are consistently higher than the measured values: the magnitudes of the calculated electric dipole matrix elements of HD are greater than the measured ones. This fact affected the values of the fit parameters B_0 and $\Delta''I$ of Table I, since in Eq. (27) the weights of the Lorentzian and the dispersion profiles are given by the products $c_0 B_0$ and $c_0\Delta''I$, respectively. An alternative approach would be to compare the computed and measured values of these products instead.

IV. CONCLUSION

The infrared-absorption R lines in the fundamental and translational bands of HD are computed, taking into account single binary collisions between HD and He at the temperature of 77 K. This is done by means of close-coupling calculations that allow for inclusion of the anisotropic interaction potential so that rotational level mixing is accounted for. The signatures arising from the interference between the permanent dipole moment of HD and the collision-induced dipole moment are investigated for four R lines. Since only single binary collisions are here considered the model is expected to describe the absorption process well only for the case of low helium density. Accordingly, a comparison with measurements has been done for low He densities either through an extrapolation of the experimentally determined Fano profile, or through a comparison of fit parameters of a low He density version of the Fano profile. Agreement between theory and measurements is observed, which seems to

TABLE II. Comparison of calculated and measured values of c_0 given in cm^{-1} am^{-1}. The measured values are taken from Refs. [11] and [5] for the R_0 lines and the R_1 lines, respectively. Square brackets indicate powers of ten.

	$R_0(0)$	$R_0(1)$	$R_1(0)$	$R_1(1)$
Calculation [29]	0.406[−5]	0.182[−5]	0.213[−7]	0.924[−8]
Measurement	0.294[−5]	0.151[−5]	0.189(9)[−7]	0.80(11)[−8]

suggest that perturbative treatments of the rotational level mixing used elsewhere are not sufficient.

The exceptionally small permanent dipole moment of the HD molecule makes the HD-He pair a quite special system for studying interference between permanent and collision-induced dipole moments in the spectrum. However, in more common cases when the permanent dipole completely dominates, the approach outlined in Sec. II can be applied, as pointed out in Ref. [32], for accurate calculations of the binary contribution to collisional line broadening.

[1] H. L. Welsh, in *Spectroscopy*, edited by A. D. Buckingham and D. A. Ramsay, MTP International Review of Science—Physical Chemistry, Series One, Vol. III (Butterworths, London, 1972), Chap. 3, pp. 33–71.

[2] L. Frommhold, *Collision-induced Absorption in Gases* (Cambridge University Press, Cambridge, 1993).

[3] A. R. W. McKellar, Can. J. Phys. **51**, 389 (1973).

[4] R. M. Herman, R. H. Tipping, and J. D. Poll, Phys. Rev. A **20**, 2006 (1979).

[5] N. H. Rich and A. R. W. McKellar, Can. J. Phys. **61**, 1648 (1983).

[6] A. R. W. McKellar, Can. J. Phys. **52**, 1144 (1974).

[7] A. R. W. McKellar, J. W. C. Johns, W. Majewski, and N. H. Rich, Can. J. Phys. **62**, 1673 (1984).

[8] J. D. Poll, R. H. Tipping, R. D. G. Prasad, and S. P. Reddy, Phys. Rev. Lett. **36**, 248 (1976).

[9] P. G. Drakopoulos and G. C. Tabisz, Phys. Rev. A **36**, 5556 (1987).

[10] P. G. Drakopoulos and G. C. Tabisz, Phys. Rev. A **36**, 5566 (1987).

[11] L. Ulivi, Z. Lu, and G. C. Tabisz, Phys. Rev. A **40**, 642 (1989).

[12] J. D. Poll, in *Phenomena Induced by Intermolecular Interactions*, edited by G. Birnbaum (Plenum Press, New York, 1985), pp. 677–694.

[13] R. M. Herman, in *Spectral Line Shapes*, edited by R. J. Exton (A. Deepak, Hampton, VA, 1987), Vol. 4, pp. 351–370.

[14] G. C. Tabisz, L. Ulivi, P. Drakopoulos, and Z. Lu, in *Spectral Line Shapes*, edited by L. Frommhold and J. W. Keto (AIP, New York, 1990), Vol. 6, pp. 421– 437.

[15] L. Ulivi, Z. Lu, and G. C. Tabisz, in *Collision- and Interaction-Induced Spectroscopy*, edited by G. C. Tabisz and M. N. Neuman (Kluwer, Dordrecht, 1995), pp. 407–416.

[16] B. McQuarrie and G. C. Tabisz, in *Spectral Line Shapes*, edited by M. Zoppi and L. Ulivi (AIP, Woodbury, NY, 1997), Vol. 9, pp. 507–510.

[17] R. M. Herman, Phys. Rev. Lett. **42**, 1206 (1979).

[18] B. Gao, G. C. Tabisz, M. Trippenbach, and J. Cooper, Phys. Rev. A **44**, 7379 (1991).

[19] M. Gustafsson, L. Frommhold, and W. Meyer, J. Chem. Phys. **113**, 3641 (2000).

[20] R. M. Herman and J. C. Lewis, in *Spectral Line Shapes*, edited by J. Seidel (AIP, Melville, NY, 2000), Vol. 11.

[21] F. H. Mies, P. S. Julienne, and K. M. Sando, COUPLE (unpublished).

[22] B. P. Stoicheff, Can. J. Phys. **35**, 730 (1957).

[23] W. A. Lester, Comput. Phys. **10**, 211 (1971).

[24] R. N. Zare, *Angular Momentum, Understanding Spatial Aspects in Chemistry and Physics* (Wiley, New York, 1988).

[25] W. Meyer, P. C. Hariharan, and W. Kutzelnigg, J. Chem. Phys. **73**, 1880 (1980).

[26] J. Schaefer and W. E. Koehler, Physica A **129**, 469 (1985).

[27] J. L. Hunt and J. D. Poll, Can. J. Phys. **56**, 950 (1978).

[28] J. D. Poll and J. L. Hunt, Can. J. Phys. **54**, 461 (1976).

[29] W. R. Thorson, J. H. Choi, and S. K. Knudson, Phys. Rev. A **31**, 34 (1985).

[30] A. Borysow, L. Frommhold, and W. Meyer, J. Chem. Phys. **88**, 4855 (1988).

[31] A. R. W. McKellar and N. H. Rich, Can. J. Phys. **62**, 1665 (1984).

[32] P. S. Julienne, Phys. Rev. A **26**, 3299 (1982).

[33] B. Gao, J. Cooper, and G. C. Tabisz, Phys. Rev. A **46**, 5781 (1992).

[34] B. McQuarrie and G. C. Tabisz, J. Mol. Liq. **70**, 159 (1996).